ARTICLE

Ets-2 deletion in myeloid cells attenuates IL-1α-mediated inflammatory disease caused by a *Ptpn6* point mutation

Sarang Tartey[1], Prajwal Gurung[1,2], Rajendra Karki[1], Amanda Burton[1], Paul Hertzog[3] and Thirumala-Devi Kanneganti[1]

The SHP-1 protein encoded by the *Ptpn6* gene has been extensively studied in hematopoietic cells in the context of inflammation. A point mutation in this gene (*Ptpn6*^{spin}) causes spontaneous inflammation in mice, which has a striking similarity to neutrophilic dermatoses in humans. Recent findings highlighted the role of signaling adapters and kinases in promoting inflammation in *Ptpn6*^{spin} mice; however, the underlying transcriptional regulation is poorly understood. Here, we report that SYK is important for driving neutrophil infiltration and initiating wound healing responses in *Ptpn6*^{spin} mice. Moreover, we found that deletion of the transcription factor *Ets2* in myeloid cells ameliorates cutaneous inflammatory disease in *Ptpn6*^{spin} mice through transcriptional regulation of its target inflammatory genes. Furthermore, Ets-2 drives IL-1α-mediated inflammatory signaling in neutrophils of *Ptpn6*^{spin} mice. Overall, in addition to its well-known role in driving inflammation in cancer, Ets-2 plays a major role in regulating IL-1α-driven *Ptpn6*^{spin}-mediated neutrophilic dermatoses.

Keywords: Autoinflammation; ETS-2; IL-1α; Neutrophilic dermatoses; PTPN6; SHP-1

Cellular & Molecular Immunology (2021) 18:1798–1808; https://doi.org/10.1038/s41423-020-0398-7

INTRODUCTION

Neutrophilic dermatoses are autoinflammatory skin conditions characterized by infiltration of neutrophils and granulocytes in the affected tissue with no evidence of infection or vasculitis.[1] The classification of neutrophilic dermatoses is complex and is based upon the recognition of clinical and pathologic features, as well as the identification of associated diseases.[2] Protein tyrosine phosphatase non-receptor type 6 (*Ptpn6*) splice variants in human patients have been linked to neutrophilic dermatoses.[3] The lack of Src homology region 2 (SH2) domain-containing phosphatase-1 (SHP-1) encoded by the *Ptpn6* gene in T cells and macrophages is associated with psoriasis[4] and multiple sclerosis,[5] respectively. SHP-1 deficiency in macrophages of patients with multiple sclerosis leads to gene expression changes driving disease pathogenesis. Altered expression of SHP-1 has also been linked to human allergies and asthmatic diseases, suggesting a role for SHP-1 in mast cells in the development of allergic inflammatory responses.[6]

A number of *Ptpn6* mutant mice with variable degrees of disease penetrance have been produced to date. *Ptpn6*$^{me/me}$ (motheaten) mice, which carry null or hypomorphic alleles of *Ptpn6*, present with severe systemic inflammation and survive up to 4 weeks.[7] *Ptpn6*$^{me\text{-}v/me\text{-}v}$ (motheaten-viable, with a T-to-A transversion at a splice consensus site) mice develop myeloproliferative disease and survive up to 10 weeks.[8] *Ptpn6*$^{meb2/meb2}$ (insertion of a B2 element into exon 6 of the *Ptpn6* gene) mice develop autoinflammatory diseases and are able to survive up to 8 months.[9] Strikingly, hypomorphic *Ptpn6*^{spin} (spontaneous inflammation, with a Tyr208Asn missense mutation in the carboxy terminus of SHP-1) mice can survive for a year and display milder symptoms than *Ptpn6*$^{me/me}$ (motheaten) mice.[10]

Ptpn6 is also known to negatively regulate interleukin-1 receptor (IL-1R)/Toll-like receptor (TLR)-mediated production of proinflammatory cytokines by suppressing the activation of mitogen-activated protein kinases (MAPKs) and the transcription factor nuclear factor κB (NF-κB).[11] Previous studies by our group have highlighted the importance of IL-1α, downstream kinases (receptor-interacting serine/threonine-protein kinase 1 [RIPK1], transforming growth factor β-activating kinase 1 [TAK1], spleen tyrosine kinase [SYK], apoptosis signal-regulating kinase 1 [ASK1]) and adapter molecules (MyD88 and caspase recruitment domain-containing protein 9 [CARD9]) in driving neutrophilic footpad inflammation independent of inflammasome activation.[12–15] We and others have also demonstrated the role of SYK in promoting inflammatory disease in *Ptpn6*^{spin} mice.[12,16] Although myeloid cell-specific deficiency of SYK in *Ptpn6*^{spin} mice provides substantial protection from inflammation, the underlying mechanism remains unexplored.

SYK, a non-receptor tyrosine kinase, is mainly expressed in the hematopoietic cell lineage[17] and plays a role in signal transduction for several tyrosine kinase-coupled receptors, including β_2-integrins and various Fc-receptors,[18,19] thereby regulating NF-κB signaling.[20,21] It has been shown that the SYK promoter contains binding sites for the transcription factors c-Jun (AP-1) and E26 avian leukemia oncogene 2, 3′ domain (Ets-2).[22] In patients with systemic lupus erythematosus, this interaction leads to increased expression of SYK, contributing to higher calcium influx in T cells.[23] Ets-2 is a well-known ubiquitous transcription factor

[1]Department of Immunology, St. Jude Children's Research Hospital, Memphis, TN 38105, USA; [2]Inflammation Program, University of Iowa, Iowa City, IA 52241, USA and [3]Centre for Innate Immunity & Infectious Diseases, Hudson Institute of Medical Research, Department of Molecular and Translational Sciences, Monash University, Clayton, Victoria 3168, Australia
Correspondence: Thirumala-Devi Kanneganti (Thirumala-Devi.Kanneganti@StJude.org)

Received: 27 November 2019 Accepted: 26 February 2020
Published online: 19 March 2020

activated after phosphorylation at threonine-72.[24] Although the role of Ets-2 in promoting oncogenesis has been widely studied, its role in inflammatory diseases is poorly understood. Given that Ets-2 can bind to the SYK promoter to modulate its expression in T cells and that activated Ets-2 is required for persistent inflammatory responses in mice carrying the motheaten viable (*me-v*) allele of the *Ptpn6* gene,[24] we hypothesized that the inflammatory disease observed in *Ptpn6*^{spin} mice could also be driven by Ets-2-mediated transcriptional programming of its target genes in myeloid cells.

In the current study, we report that SYK or Ets-2 deletion in macrophages or neutrophils of *Ptpn6*^{spin} mice significantly rescues cutaneous inflammatory disease by ameliorating neutrophil infiltration in the footpads and draining lymph nodes. Collectively, the results demonstrate that Ets-2- and SYK-mediated signaling pathways play critical roles in eliciting *Ptpn6*^{spin}-mediated inflammation by regulating the transcription of inflammatory signaling molecules.

RESULTS

SYK promotes disease in *Ptpn6*^{spin} mice by inducing neutrophil-mediated proinflammatory cytokine and chemokine production

Our recent study demonstrated that SYK is a critical kinase that is centrally required for the induction of inflammatory disease in *Ptpn6*^{spin} mice.[12] To explore the underlying mechanism, we performed a detailed investigation using *Ptpn6*^{spin} mice with a myeloid-specific deletion of SYK (*Ptpn6*^{spin}*Syk*$^{fl/fl}$*LysM*$^{Cre+}$ mice) and mice with a neutrophil-specific deletion of *Ptpn6* and *Syk* (*Ptpn6*$^{fl/fl}$*Syk*$^{fl/fl}$*S100a8*$^{Cre+}$ mice). Previous studies have reported that *Ptpn6*^{spin}*Syk*$^{fl/fl}$*LysM*$^{Cre+}$ and *Ptpn6*$^{fl/fl}$*Syk*$^{fl/fl}$*S100a8*$^{Cre+}$ mice have a significant delay in disease progression compared with *Ptpn6*^{spin} and *Ptpn6*$^{fl/fl}$*S100a8*$^{Cre+}$ mice, respectively.[12,16] Given that inflammation in *Ptpn6*^{spin} mice is characterized by the infiltration of neutrophils,[14] we performed neutrophil-specific immunostaining on footpad sections. This staining showed severe neutrophilia in *Ptpn6*^{spin} and *Ptpn6*$^{fl/fl}$*S100a8*$^{Cre+}$ mice, and this neutrophilia was completely rescued in the *Ptpn6*^{spin}*Syk*$^{fl/fl}$*LysM*$^{Cre+}$ and *Ptpn6*$^{fl/fl}$*Syk*$^{fl/fl}$*S100a8*$^{Cre+}$ mice (Fig. 1a, b). These data suggest that SYK deletion in the myeloid cell compartment, specifically in neutrophils, is sufficient to provide significant protection in *Ptpn6*^{spin} mice.

Neutrophils are known to respond to a variety of signals by producing cytokines and other inflammatory factors to regulate inflammation.[25] The increase in cytokine levels at the site of inflammation is associated with an increase in the number of circulating neutrophils in the peripheral blood. While *Ptpn6*^{spin} and *Ptpn6*$^{fl/fl}$*S100a8*$^{Cre+}$ mice presented with increased cytokine and chemokine levels, including granulocyte colony-stimulating factor (G-CSF), IL-6 and CXCL1 chemokine KC (KC/CXCL-1), in the serum and footpads, the levels of these cytokines and chemokines were significantly reduced in the serum and footpads of *Ptpn6*^{spin}*Syk*$^{fl/fl}$*LysM*$^{Cre+}$ and *Ptpn6*$^{fl/fl}$*Syk*$^{fl/fl}$*S100a8*$^{Cre+}$ mice, respectively (Fig. 1c, d; Supplementary Fig. 1a, b). These results indicate that SYK plays an important role in *Ptpn6*^{spin}-mediated inflammation by regulating inflammatory cytokine and chemokine production.

SYK in neutrophils regulates IL-1α-mediated inflammatory signaling in *Ptpn6*^{spin} and *Ptpn6*$^{fl/fl}$*S100a8*$^{Cre+}$ mice

IL-1α is constitutively expressed in many cell types, and its expression increases in response to inflammatory stimuli.[26] This "sterile inflammation" may lead to immune dysfunction and overall disease pathogenesis. We have previously shown that IL-1α drives inflammation in *Ptpn6*^{spin} mice by exacerbating inflammatory signaling in neutrophils.[13] To understand the role of SYK in IL-1α-mediated inflammation in *Ptpn6*^{spin} mice, we stimulated neutrophils from pre-diseased *Ptpn6*^{spin} mice with recombinant IL-1α and analyzed the activation status of NF-κB and MAPK signaling. Consistent with previous results,[14,15] IL-1α stimulation led to increased phosphorylation of IκBα, Erk1/2 and p38 in neutrophils from pre-diseased *Ptpn6*^{spin} mice compared with neutrophils from wild-type mice (Fig. 2a). Neutrophils from *Ptpn6*$^{fl/fl}$*S100a8*$^{Cre+}$ mice also showed hyperactivation of NF-κB and MAPK signaling upon IL-1α stimulation compared with neutrophils from *Ptpn6*$^{fl/fl}$*S100a8*$^{Cre−}$ mice (Fig. 2b). Notably, the enhanced inflammatory signaling was rescued in neutrophils from *Ptpn6*^{spin}*Syk*$^{fl/fl}$*LysM*$^{Cre+}$ and *Ptpn6*$^{fl/fl}$*Syk*$^{fl/fl}$*S100a8*$^{Cre+}$ mice (Fig. 2a, b; Supplementary Fig. 2a, b), suggesting that neutrophilic SYK plays a role in regulating IL-1α-driven inflammation in mice with mutant *Ptpn6*.

IL-1α is also well-known as an alarm signal to initiate inflammation in response to tissue injury, leading to massive cell necrosis.[27] Therefore, we next tested whether the defective wound healing responses observed in *Ptpn6*^{spin} mice can be rescued in the absence of SYK. We performed microabrasion on the plantar surface of the hind feet and monitored for the induction of inflammatory cytokines and chemokines (6 h post-wound induction). In accordance with our previous studies,[12,13] wild-type mice showed secretion of proinflammatory cytokines (G-CSF, IL-6) and chemokines (CXCL1/KC, MCP-1), and this secretion was exacerbated in *Ptpn6*^{spin} and *Ptpn6*$^{fl/fl}$*S100a8*$^{Cre+}$ mice (Fig. 2c, d). This enhanced secretion of inflammatory factors was fully rescued in *Ptpn6*^{spin}*Syk*$^{fl/fl}$*LysM*$^{Cre+}$ and *Ptpn6*$^{fl/fl}$*Syk*$^{fl/fl}$*S100a8*$^{Cre+}$ mice (Fig. 2c, d). Taken together, these results highlight a critical role for SYK in driving both IL-1α-induced sterile inflammation and wound healing responses in *Ptpn6*^{spin} and *Ptpn6*$^{fl/fl}$*S100a8*$^{Cre+}$ mice.

Deletion of Ets-2 in myeloid cells ameliorates cutaneous inflammatory disease in *Ptpn6*^{spin} mice

Previous work has shown that the *Syk* promoter contains binding sites for the transcription factors c-Jun (AP-1) and Ets-2.[22] Given that Ets-2 contributes to the upregulation of SYK in activated T cells,[22] we hypothesized that *Syk* expression in neutrophils can also be regulated by *Ets2*. The basal *Syk* mRNA expression was reduced in neutrophils from wild-type mice compared with those from *Ets2*$^{fl/fl}$*LysM*$^{Cre+}$ mice (Fig. 3a). Based on this lower expression of *Syk* in *Ets2*$^{fl/fl}$*LysM*$^{Cre+}$ neutrophils and because SYK phosphorylation drives inflammatory disease in *Ptpn6*^{spin} mutant mice,[12] we next investigated the levels of *Ets2* mRNA in neutrophils harvested from *Ptpn6*^{spin} mutant mice. *Ets2* mRNA expression was substantially increased in these neutrophils compared with that in wild-type mice (Fig. 3b). These data suggest a link between Ets-2 and the transcriptional regulation of *Syk* and its target genes to modulate the inflammatory responses in *Ptpn6*^{spin} mice.

To further investigate the role of Ets-2 in *Ptpn6*^{spin}-mediated pathology, we generated *Ptpn6*^{spin}*Ets2*$^{fl/fl}$*LysM*$^{Cre+}$ mice by crossing *Ets2*$^{fl/fl}$*LysM*$^{Cre+}$ mice[28] with *Ptpn6*^{spin} mice. Consistent with our previous findings,[12–15] *Ptpn6*^{spin} mice spontaneously developed footpad inflammation at 6–10 weeks of age. However, *Ptpn6*^{spin}*Ets2*$^{fl/fl}$*LysM*$^{Cre+}$ mice were significantly protected from inflammatory disease progression compared with *Ptpn6*^{spin} mice. All the protected mice remained disease free until study termination (20 weeks) with no evident signs of footpad swelling or inflammation (Fig. 3c, d). Next, we performed histological analysis of the footpads of wild-type, *Ptpn6*^{spin} and *Ptpn6*^{spin}*Ets2*$^{fl/fl}$*LysM*$^{Cre+}$ mice. Histological analysis confirmed that the extent of inflammation and lesions were attenuated in *Ptpn6*^{spin}*Ets2*$^{fl/fl}$*LysM*$^{Cre+}$ mice compared with *Ptpn6*^{spin} mice (Fig. 3e). Immunohistochemical analysis with neutrophil-specific immunostaining revealed severe neutrophilia in *Ptpn6*^{spin} mice, and this neutrophilia was completely rescued in the footpads of *Ptpn6*^{spin}*Ets2*$^{fl/fl}$*LysM*$^{Cre+}$ mice (Fig. 3f). These findings suggest that myeloid cell-specific Ets-2 drives neutrophilic footpad inflammation in *Ptpn6*^{spin} mice.

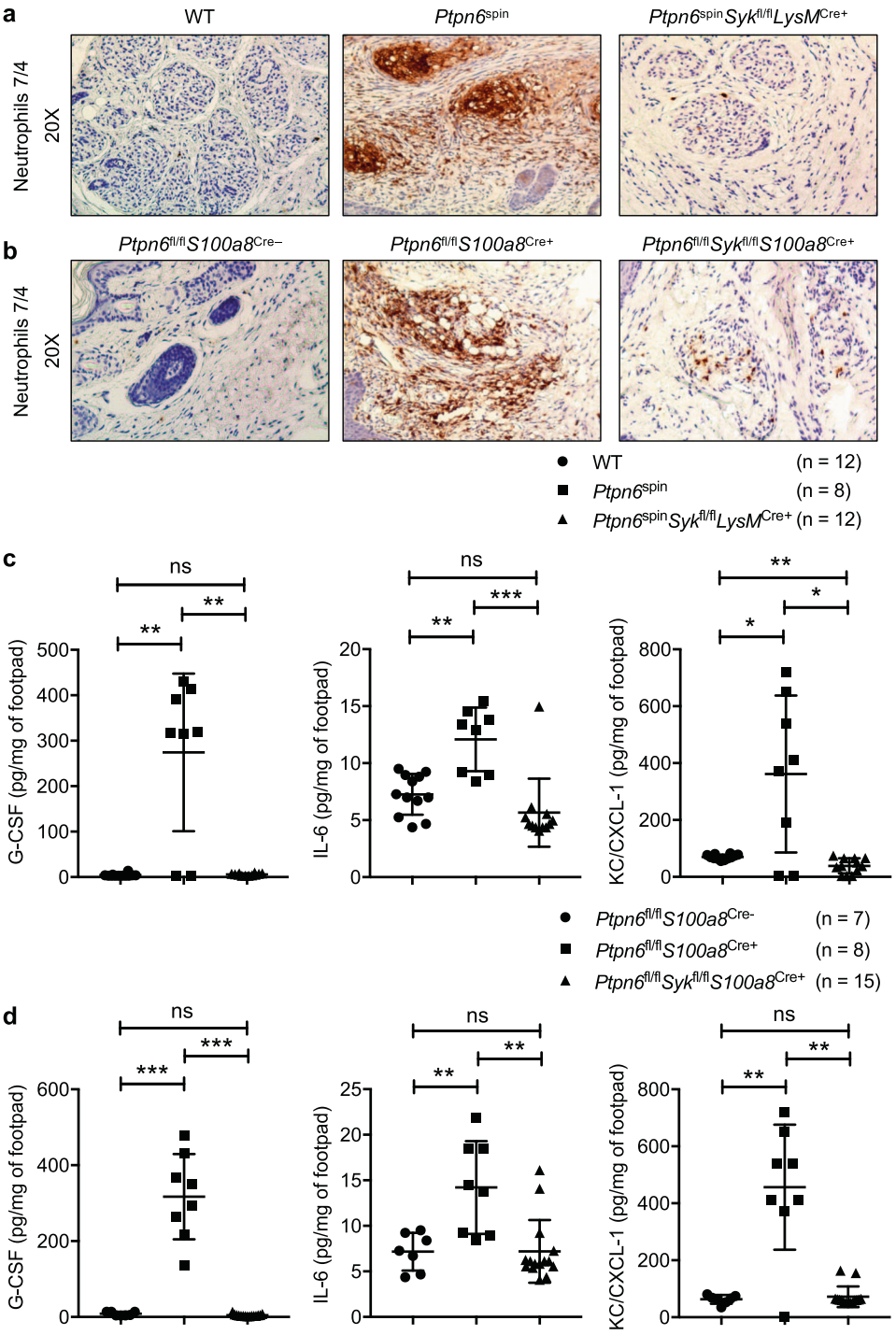

Fig. 1 SYK promotes disease in *Ptpn6*^{spin} mice by inducing neutrophil-mediated proinflammatory cytokine and chemokine production. **a** Footpads from wild-type (WT), *Ptpn6*^{spin} and *Ptpn6*^{spin}*Syk*$^{fl/fl}$*LysM*$^{Cre+}$ mice were harvested and subjected to immunohistochemical staining for neutrophils (anti-neutrophil antibody 7/4). **b** Footpads from *Ptpn6*$^{fl/fl}$*S100a8*$^{Cre–}$, *Ptpn6*$^{fl/fl}$*S100a8*$^{Cre+}$ and *Ptpn6*$^{fl/fl}$*Syk*$^{fl/fl}$*S100a8*$^{Cre+}$ mice were harvested and subjected to immunohistochemical staining for neutrophils (anti-neutrophil antibody 7/4). **c** Footpads from WT ($n = 12$), *Ptpn6*^{spin} ($n = 8$) and *Ptpn6*^{spin}*Syk*$^{fl/fl}$*LysM*$^{Cre+}$ ($n = 12$) mice were homogenized, and the concentrations of cytokines (G-CSF, IL-6) and the chemokine KC/CXCL-1 were measured by ELISA in the quantified lysates. **d** Footpads from *Ptpn6*$^{fl/fl}$*S100a8*$^{Cre–}$ ($n = 7$), *Ptpn6*$^{fl/fl}$*S100a8*$^{Cre+}$ ($n = 8$) and *Ptpn6*$^{fl/fl}$*Syk*$^{fl/fl}$*S100a8*$^{Cre+}$ ($n = 15$) mice were homogenized, and the concentrations of cytokines (G-CSF, IL-6) and the chemokine KC/CXCL-1 were measured by ELISA in the quantified lysates. Each point represents an individual mouse, and the lines represent the mean ± SD. The unpaired *t* test with Welch's correction was used to determine the significance between the two groups analyzed. ns, not significant; *$P < 0.05$; **$P < 0.01$; ***$P < 0.001$

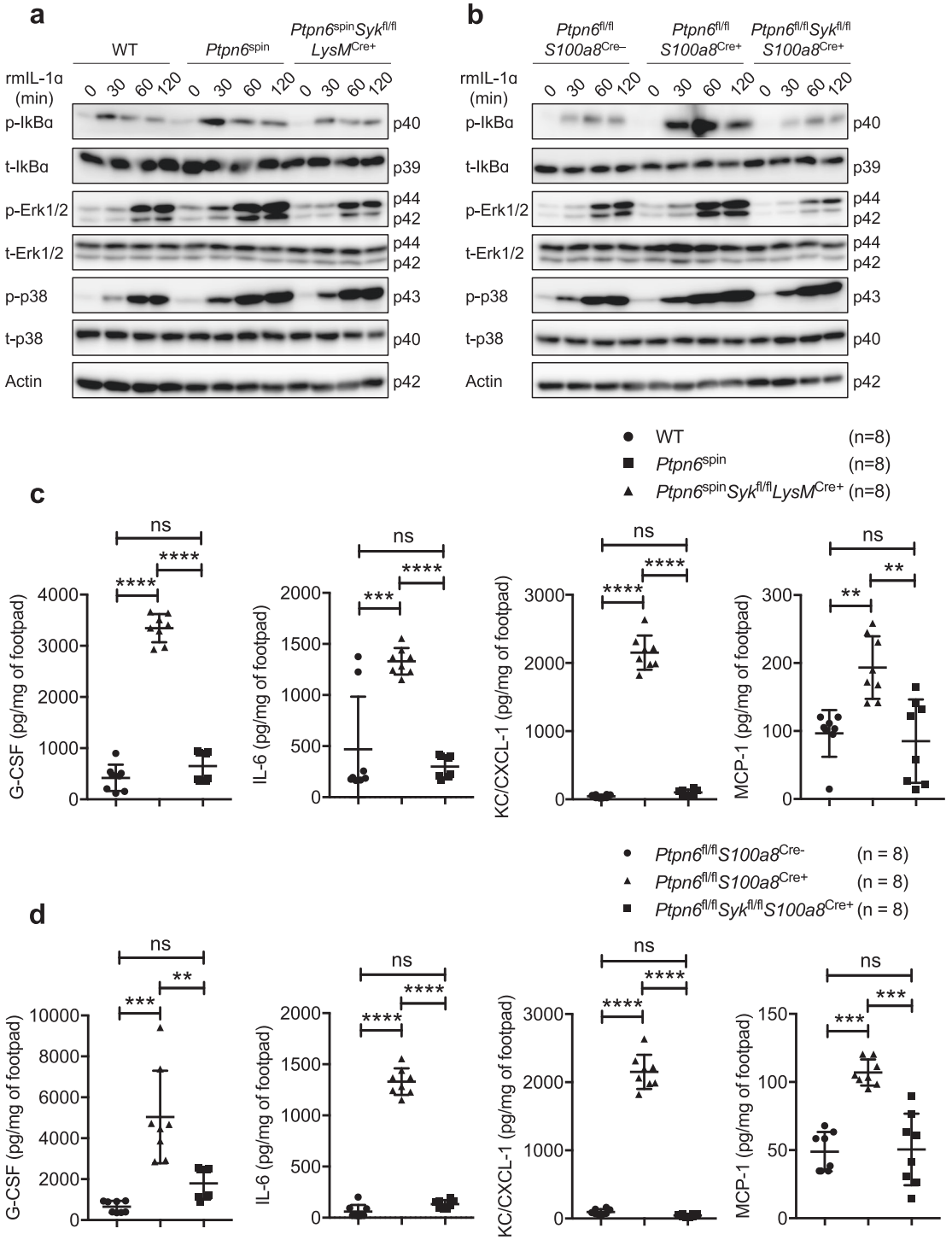

Fig. 2 SYK in neutrophils regulates IL-1α-mediated inflammatory signaling in *Ptpn6*^{spin} and *Ptpn6*$^{fl/fl}$*S100a8*$^{Cre+}$ mutant mice. **a** Neutrophils from the bone marrow of wild-type (WT), pre-diseased *Ptpn6*^{spin} and *Ptpn6*^{spin}*Syk*$^{fl/fl}$*LysM*$^{Cre+}$ mice were harvested and stimulated with recombinant mouse IL-1α (rmIL-1α; 10 ng/mL) for the indicated time period. Whole-cell lysates were prepared, and the protein levels of phosphorylated (p)-IκBα, total (t)-IκBα, p-Erk1/2, t-Erk1/2, p-p38 and t-p38 were determined by western blotting. β-Actin was used as an internal control. **b** Neutrophils from the bone marrow of *Ptpn6*$^{fl/fl}$*S100a8*$^{Cre-}$, pre-diseased *Ptpn6*$^{fl/fl}$*S100a8*$^{Cre+}$ and *Ptpn6*$^{fl/fl}$*Syk*$^{fl/fl}$*S100a8*$^{Cre+}$ mice were harvested and stimulated with rmIL-1α (10 ng/mL) for the indicated time period. Whole-cell lysates were prepared, and the protein levels of p-IκBα, t-IκBα, p-Erk1/2, t-Erk1/2, p-p38 and t-p38 were determined by western blotting. β-Actin was used as an internal control. **c** Footpads from WT ($n = 8$), *Ptpn6*^{spin} ($n = 8$) and *Ptpn6*^{spin}*Syk*$^{fl/fl}$*LysM*$^{Cre+}$ ($n = 8$) mice were microabrated, and the concentrations of G-CSF, IL-6, KC/CXCL-1 and MCP-1 were measured in the footpads 6 h post-microabrasion. **d** Footpads from *Ptpn6*$^{fl/fl}$*S100a8*$^{Cre-}$ ($n = 8$), *Ptpn6*$^{fl/fl}$*S100a8*$^{Cre+}$ ($n = 8$) and *Ptpn6*$^{fl/fl}$*Syk*$^{fl/fl}$*S100a8*$^{Cre+}$ ($n = 8$) mice were microabrated, and the concentrations of G-CSF, IL-6, KC/CXCL-1 and MCP-1 were measured in the footpads 6 h post-microabrasion. Each point represents an individual mouse, and the lines represent the mean ± SD. Two-way ANOVA with Tukey's multiple comparisons test was used to determine the significance between the two groups analyzed. ns not significant; $^{**}P < 0.01$; $^{***}P < 0.001$; $^{****}P < 0.0001$

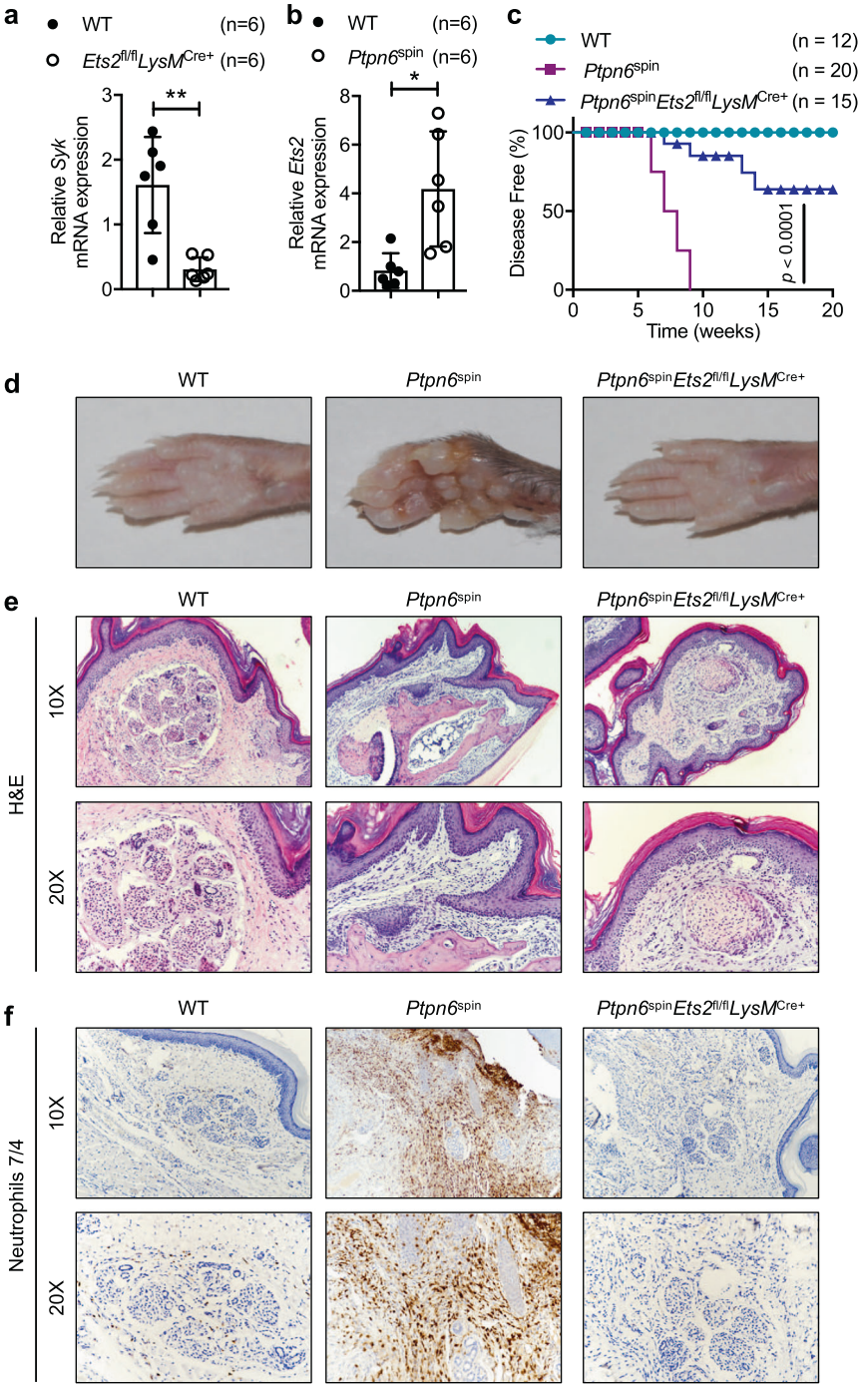

Fig. 3 Deletion of Ets-2 in myeloid cells ameliorates cutaneous inflammatory disease in *Ptpn6*^{spin} mice. **a** Neutrophils from bone marrow of wild-type (WT) ($n = 6$) and *Ets2*$^{fl/fl}$*LysM*$^{Cre+}$ ($n = 6$) mice were harvested. After RNA isolation, qPCR was performed to determine the mRNA expression of *Syk*. Expression was normalized to that of *Gapdh*. **b** Neutrophils from bone marrow of WT ($n = 6$) and *Ptpn6*^{spin} ($n = 6$) mice were harvested. After RNA isolation, qPCR was performed to determine the mRNA expression of *Ets2*. Expression was normalized to that of *Gapdh*. **c** WT ($n = 12$), *Ptpn6*^{spin} ($n = 20$) and *Ptpn6*^{spin}*Ets2*$^{fl/fl}$*LysM*$^{Cre+}$ ($n = 15$) mice were observed for disease progression. **d** Representative footpad images from WT, *Ptpn6*^{spin} and *Ptpn6*^{spin}*Ets2*$^{fl/fl}$*LysM*$^{Cre+}$ mice. **e**, **f** Footpads from WT, *Ptpn6*^{spin} and *Ptpn6*^{spin}*Ets2*$^{fl/fl}$*LysM*$^{Cre+}$ mice were harvested and subjected to **e** hematoxylin and eosin (H&E) and **f** immunohistochemical staining of neutrophils (anti-neutrophil antibody 7/4) (Magnification: 10× and 20×). Data are presented as the mean ± SD. The unpaired *t* test with Welch's correction was used to determine the statistical significance of the gene expression data. Disease progress curves in (**c**) were analyzed by the log-rank (Mantel-Cox) test. *$P < 0.05$; **$P < 0.01$

Ets-2 deletion attenuates the infiltration of myeloid cells observed in *Ptpn6*^{spin} mice

Since *Ptpn6*^{spin} mice are characterized by enlarged spleens and popliteal lymph nodes (pLNs) that drain the inflamed feet, we analyzed the spleens and pLNs from *Ptpn6*^{spin}*Ets2*$^{fl/fl}$*LysM*$^{Cre+}$ mice. In line with the observed rescue of footpad inflammation, *Ptpn6*^{spin}*Ets2*$^{fl/fl}$*LysM*$^{Cre+}$ mice showed normal spleens and pLNs (Fig. 4a), comparable to those of wild-type mice. Further analysis revealed that the increase in cell numbers in the spleens and pLNs observed in *Ptpn6*^{spin} mice was substantially rescued in

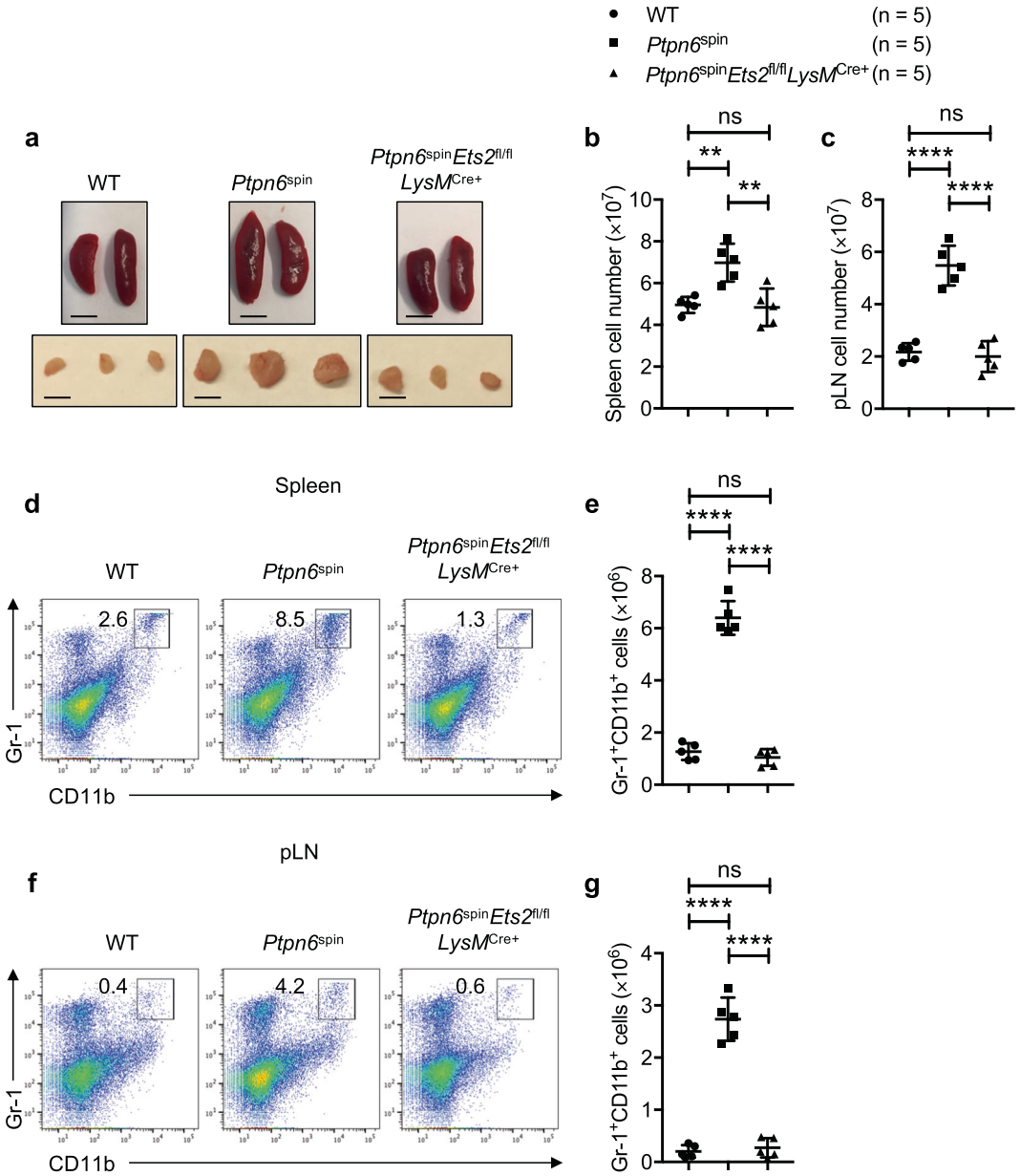

Fig. 4 Ets-2 deletion attenuates the infiltration of myeloid cells observed in *Ptpn6*^{spin} mice. **a** Representative images of spleens and popliteal lymph nodes (pLNs) from wild-type (WT), *Ptpn6*^{spin} and *Ptpn6*^{spin}*Ets2*$^{fl/fl}$*LysM*$^{Cre+}$ mice; scale bar (5 mm). **b**, **c** Cell numbers in **b** the spleen and **c** pLN from WT ($n = 5$), *Ptpn6*^{spin} ($n = 5$) and *Ptpn6*^{spin}*Ets2*$^{fl/fl}$*LysM*$^{Cre+}$ ($n = 5$) mice. **d**, **e** Flow cytometry analysis of the Gr-1^{+}CD11b^{+} neutrophil population in the spleen of WT ($n = 5$), *Ptpn6*^{spin} ($n = 5$) and *Ptpn6*^{spin}*Ets2*$^{fl/fl}$*LysM*$^{Cre+}$ ($n = 5$) mice. **f**, **g** Flow cytometry analysis of the Gr-1^{+}CD11b^{+} neutrophil population in the pLN of WT ($n = 5$), *Ptpn6*^{spin} ($n = 5$) and *Ptpn6*^{spin}*Ets2*$^{fl/fl}$*LysM*$^{Cre+}$ ($n = 5$) mice. Each point represents an individual mouse, and the lines represent the mean ± SD. The unpaired *t* test was used to determine the significance between the two groups analyzed. ns not significant; $^{**}P < 0.01$; $^{****}P < 0.0001$

Ptpn6^{spin}*Ets2*$^{fl/fl}$*LysM*$^{Cre+}$ mice (Fig. 4b, c). Flow cytometric analysis of cells from *Ptpn6*^{spin}*Ets2*$^{fl/fl}$*LysM*$^{Cre+}$ mice showed that the percentages and total numbers of Gr-1^{+}CD11b^{+} cells in the spleen (Fig. 4d, e) and pLN (Fig. 4f, g) tended to be consistent with those of wild-type mice and were significantly lower than the levels in *Ptpn6*^{spin} mice. These data indicate that an Ets-2-dependent increase in the numbers of infiltrating myeloid cells is associated with inflammatory disease in *Ptpn6*^{spin} mice.

Ets-2 regulates transcriptional control of inflammatory genes in *Ptpn6*^{spin} mice

To further define the molecular basis underlying the attenuation of inflammatory responses observed in *Ptpn6*^{spin}*Ets2*$^{fl/fl}$*LysM*$^{Cre+}$ mice, we performed quantitative polymerase chain reaction (qPCR) analysis to study the gene expression changes in the footpads of wild-type, *Ptpn6*^{spin} and *Ptpn6*^{spin}*Ets2*$^{fl/fl}$*LysM*$^{Cre+}$ mice. We analyzed a set of well-defined Ets-2 target genes including matrix metalloproteinase 9 (*Mmp9*) and genes involved in inflammatory responses (*Il6* and *Tnf*). In addition, we also analyzed genes known to have Ets binding sites in their promoters, such as the cytokine gene *Il1a* and the chemokine genes *Ccl3* and *Ccl4*. Expression of *Mmp9*, *Il6* and *Tnf* was highly induced in the footpads and pLNs of *Ptpn6*^{spin} mice compared with the expression in wild-type mice, and this enhanced gene expression was found to be reduced in the *Ptpn6*^{spin}*Ets2*$^{fl/fl}$*LysM*$^{Cre+}$ mice (Fig. 5a, b). Similar to the expression pattern of the known Ets-2 target genes, the gene

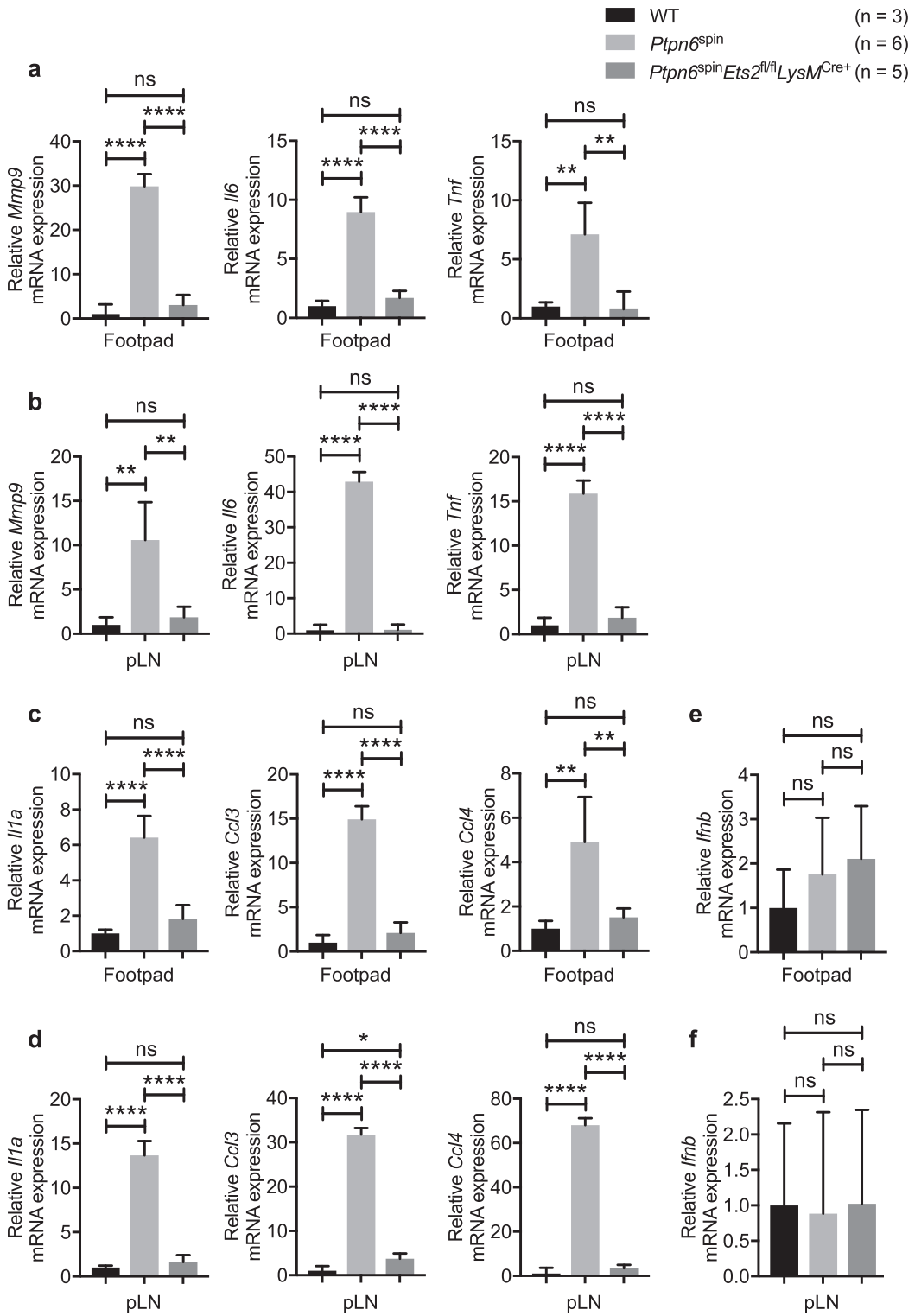

Fig. 5 Ets-2 regulates the expression of inflammatory genes in *Ptpn6*^{spin} mice. **a**–**f** Footpads and popliteal lymph nodes (pLNs) were harvested from wild-type (WT) ($n = 3$), *Ptpn6*^{spin} ($n = 6$) and *Ptpn6*^{spin}*Ets2*$^{fl/fl}$*LysM*$^{Cre+}$ ($n = 5$) mice. RNA was isolated, and qPCR was performed to analyze the mRNA expression of the known Ets-2 target genes **a**, **b** *Mmp9*, *Il6*, *Tnf* and the genes containing Ets-2 binding sites in their promoters **c**, **d** *Il1a*, *Ccl3*, *Ccl4*. **e**, **f** *Ifnb* was used as a negative control. Gene expression was normalized to that of *Gapdh*. Data are presented as the mean ± SD. The unpaired *t* test with Welch's correction was used to determine the statistical significance. ns, not significant; *$P < 0.05$; **$P < 0.01$; ****$P < 0.0001$

expression of *Il1a*, *Ccl3* and *Ccl4* was also found to be enhanced in the footpads and pLNs of *Ptpn6*^{spin} mice compared with the expression in wild-type mice, and this was attenuated in *Ptpn6*^{spin}*Ets2*$^{fl/fl}$*LysM*$^{Cre+}$ mice (Fig. 5c, d). Next, we measured *Ifnb* expression levels as a negative control in the footpads and pLNs of wild-type, *Ptpn6*^{spin} and *Ptpn6*^{spin}*Ets2*$^{fl/fl}$*LysM*$^{Cre+}$ mice. No apparent changes in the *Ifnb* expression levels were observed in *Ptpn6*^{spin} mice compared with wild-type and *Ptpn6*^{spin}*Ets2*$^{fl/fl}$*LysM*$^{Cre+}$ mice

(Fig. 5e, f). Taken together, these data suggest that Ets-2 regulates the transcriptional control of genes involved in inflammatory responses in *Ptpn6*^{spin} mice.

Ets-2 in myeloid cells regulates IL-1α-mediated inflammatory signaling in *Ptpn6*^{spin} mice

To investigate the role of Ets-2 in IL-1α-mediated inflammation in *Ptpn6*^{spin} mice, we harvested and stimulated neutrophils from wild-type, pre-diseased *Ptpn6*^{spin} and *Ptpn6*^{spin}*Ets2*$^{fl/fl}$*LysM*$^{Cre+}$ mice with IL-1α for the indicated amount of time. Next, we performed immunoblotting with the cell lysates to determine the activation status of NF-κB and MAPK signaling components. While the neutrophils from pre-diseased *Ptpn6*^{spin} mice stimulated with IL-1α responded with increased phosphorylation of IκBα and Erk1/2, this hyperphosphorylation was diminished in the neutrophils from pre-diseased *Ptpn6*^{spin}*Ets2*$^{fl/fl}$*LysM*$^{Cre+}$ mice (Fig. 6a; Supplementary Fig. 3a). We further examined the status of NF-κB and MAPK signaling in footpad lysates from wild-type, *Ptpn6*^{spin} and *Ptpn6*^{spin}*Ets2*$^{fl/fl}$*LysM*$^{Cre+}$ mice. In agreement with the in vitro stimulation data, we found that deletion of *Ets2* decreased NF-κB and MAPK signaling in the footpads of *Ptpn6*^{spin}*Ets2*$^{fl/fl}$*LysM*$^{Cre+}$ mice (Fig. 6b; Supplementary Fig. 3b).

We next analyzed the level of cytokine and chemokine secretion at the site of inflammation and by circulating neutrophils in the serum of wild-type, *Ptpn6*^{spin} and *Ptpn6*^{spin}*Ets2*$^{fl/fl}$*LysM*$^{Cre+}$ mice. The increased levels of G-CSF, IL-6, KC/CXCL1 and MCP-1/CCL2 observed in *Ptpn6*^{spin} mice were significantly diminished in the serum and footpads of *Ptpn6*^{spin}*Ets2*$^{fl/fl}$*LysM*$^{Cre+}$ mice (Fig. 6c, d). These results indicate that Ets-2 plays an important role in *Ptpn6*^{spin}-mediated inflammation by regulating inflammatory cytokine and chemokine production. Collectively, these results suggest that neutrophilic Ets-2 acts as a critical regulator of IL-1α-driven inflammation in *Ptpn6* mutant mice.

DISCUSSION

Protein tyrosine phosphatases are widely accepted as signaling molecules that can regulate cell growth, differentiation, the mitotic cycle and oncogenic transformation.[29] *Ptpn6* is primarily expressed in hematopoietic cells, where it regulates multiple signaling pathways.[10] *PTPN6* gene polymorphisms are associated with a wide spectrum of autoinflammatory diseases.[30,31] SHP-1 is also suggested to be involved as an insulin signaling and insulin clearance regulator in the liver and is associated with the development of diabetic retinopathy.[32,33] Recent studies, including ours, have demonstrated the role of several important molecules driving inflammatory disease in *Ptpn6*^{spin} mice.[10,12–16] Despite this enormous amount of data pointing to the critical role of *PTPN6* in cells of hematopoietic origin, very little is known about the mechanisms governing SHP-1 expression in myeloid cells, especially neutrophils.

SYK represents a common focal point in the signaling pathways of Dectin-1, Dectin-2 and TLRs.[34,35] SYK has been shown to be associated with TNF receptor-associated factor 6 (TRAF6) after IL-1 stimulation in nasal fibroblast lines,[36] and SYK can also induce MYD88 phosphorylation in response to IL-1α treatment.[12] In addition, in T cells, SYK expression has been shown to be regulated by the transcription factor Ets-2.[22] However, the steps linking SYK and Ets-2 in the context of neutrophil-mediated inflammation downstream of IL-1α are currently undefined.

Previous studies highlighted the importance of phosphorylated Ets-2 in lung inflammation and extracellular matrix remodeling, both of which are involved in pulmonary fibrosis.[37,38] In addition to its role in lung inflammation, it has been suggested that Ets-2 binds super-enhancers and reprograms gene expression to promote the development of cancer.[39] Ets-2 is a well-studied transcription factor in the context of tumorigenesis, and several Ets-2 target genes (*Mmp9*, *Tnf*, etc.) have been reported previously.[40] In addition to these well-known target genes, several cytokine and chemokine genes contain Ets-binding sites in their promoter regions (*Il1a*, *Ccl3*, *Ccl4*, etc.).

Ets2-deficient mice are embryonically lethal and die early due to defective trophoblast function.[41] In the current study, we utilized myeloid cell-specific *Ets2* conditional knockout mice[28] and found that the expression of major Ets-2 target genes is highly upregulated in the footpads and pLNs of diseased *Ptpn6*^{spin} mice. This upregulation is substantially diminished in *Ptpn6*^{spin}*Ets2*$^{fl/fl}$*LysM*$^{Cre+}$ mice. One possible explanation could be that Ets-2 binds to each of these gene promoters, including the promoter of *Il1a*, to regulate their transcriptional activity. This interaction could lead to increased IL-1α production in *Ptpn6*^{spin} mice, thereby resulting in aggravated inflammation. These data suggest that Ets-2 regulates a set of genes in myeloid cells, either directly or indirectly, that is necessary for the severe inflammatory phenotype in the *Ptpn6*^{spin} mouse model. Additional studies are needed to explore the extent of Ets-2 activation, the resulting transcriptional modifications and how they impact neutrophilic dermatoses in *Ptpn6*^{spin} mice. Whether SHP-1 regulates the transcription of Ets-2 or vice versa will be an interesting question for future studies.

Overall, we have shown that IL-1α can activate the NF-κB and MAPK signaling pathways in *Ptpn6*^{spin} mice, which is driven by SYK and Ets-2 in myeloid cells. Our data highlight a critical role for Ets-2-dependent gene transcription in a mouse model of neutrophilic dermatoses to drive an inflammatory pathway that results in excessive inflammatory responses and persistent tissue damage. Furthermore, we demonstrated that IL-1α-stimulated neutrophils require the transcription factor Ets-2 to promote inflammatory disease in *Ptpn6*^{spin} mice, since deletion of Ets-2 caused a significant reduction in neutrophilic inflammation. In summary, our study defines a previously undescribed role for Ets-2 and SYK regulation in IL-1α-mediated inflammatory disease in a mouse model of neutrophilic dermatoses. Consequently, inhibition of SYK or Ets-2 by blocking its kinase activity or phosphorylation, respectively, may provide novel approaches to effectively treat inflammatory skin disorders. This study opens avenues to further explore these pathways to study inflammatory disorders independent of infection.

METHODS

Mice

Syk$^{fl/fl}$ (ref. [42]), *Ptpn6*$^{fl/fl}$ (ref. [43]), *Ptpn6*^{spin} (ref. [10]), *LysM*$^{Cre+}$ (ref. [44]) and *S100a8*$^{Cre+}$ (ref. [45]) mice have been described previously. *Ets2*$^{fl/fl}$*LysM*$^{Cre+}$ mice were obtained from Paul Hertzog (Hudson Institute of Medical Research, Clayton, Victoria, Australia). *Ptpn6*$^{fl/fl}$*S100a8*$^{Cre+}$ mice were generated by crossing *Ptpn6*$^{fl/fl}$ mice with *S100a8*$^{Cre+}$ mice. *Ptpn6*^{spin}*Ets2*$^{fl/fl}$*LysM*$^{Cre+}$, *Ptpn6*^{spin}*Syk*$^{fl/fl}$*LysM*$^{Cre+}$ and *Ptpn6*$^{fl/fl}$*Syk*$^{fl/fl}$*S100a8*$^{Cre+}$ mice were generated by crossing *Ptpn6*^{spin} and *Ptpn6*$^{fl/fl}$*S100a8*$^{Cre+}$ mice with *Ets2*$^{fl/fl}$*LysM*$^{Cre+}$, *Syk*$^{fl/fl}$*LysM*$^{Cre+}$ and *Syk*$^{fl/fl}$ mice, respectively. Male and female 6–10-week-old mice were used in this study except in the microabrasion assays where mice as young as 4 weeks were used. Mice were housed under specific pathogen-free conditions in the Animal Resource Center at St. Jude Children's Research Hospital. All animal studies were approved by the Institutional Animal Care and Use Committee (IACUC) of St. Jude Children's Research Hospital, Memphis, TN. All the methods were performed in strict accordance with the relevant guidelines and regulations.

Neutrophil isolation and in vitro stimulation

Femurs were collected from mice, cells from the bone marrow were isolated, and neutrophils (CD11b^{+} Gr-1^{+}) were purified by fluorescence-activated cell sorting as previously described.[13,14] Purified neutrophils (1×10^{6} cells/mL) were stimulated for the indicated amount of time with recombinant murine IL-1α (10 ng/mL; Gold Biotechnology). For immunoblotting,

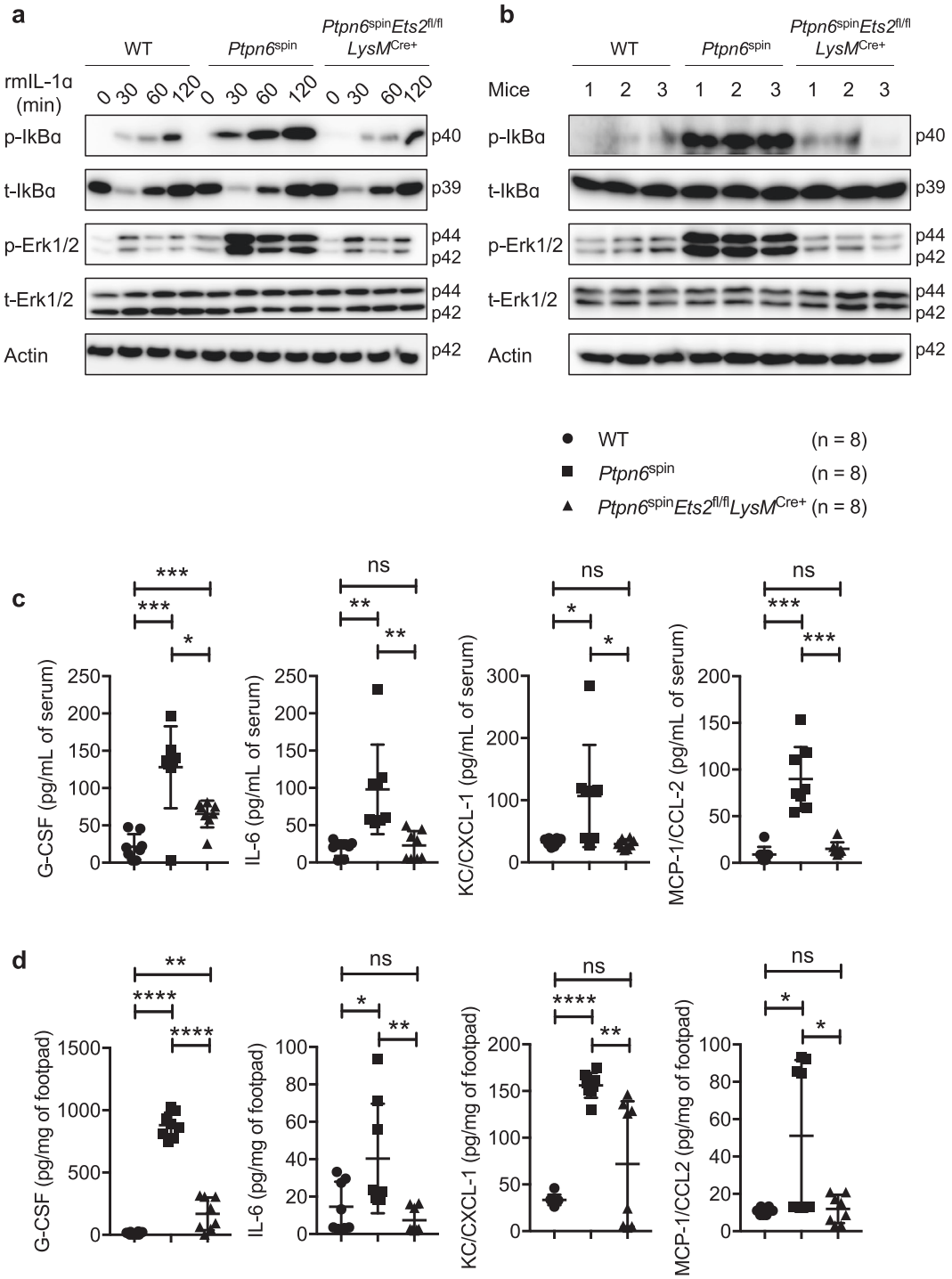

Fig. 6 Ets-2 in myeloid cells regulates IL-1α-mediated inflammatory signaling in *Ptpn6*^{spin} mice. **a** Neutrophils from the bone marrow of wild-type (WT), pre-diseased *Ptpn6*^{spin} and *Ptpn6*^{spin}*Ets2*$^{fl/fl}$*LysM*$^{Cre+}$ mice were harvested and stimulated with recombinant mouse IL-1α (rmIL-1α; 10 ng/mL) for the indicated time period. Whole-cell lysates were prepared, and the protein levels of phosphorylated (p)-IκBα, total (t)-IκBα, p-Erk1/2 and t-Erk1/2 were determined by western blotting. β-Actin was used as an internal control. **b** Footpads from WT, *Ptpn6*^{spin} and *Ptpn6*^{spin}*Ets2*$^{fl/fl}$*LysM*$^{Cre+}$ mice were homogenized, and protein levels of p-IκBα, t-IκBα, p-Erk1/2 and t-Erk1/2 were determined in quantified lysates by western blotting. β-Actin was used as an internal control. **c** Serum was harvested from WT ($n = 8$), *Ptpn6*^{spin} ($n = 8$) and *Ptpn6*^{spin}*Ets2*$^{fl/fl}$*LysM*$^{Cre+}$ ($n = 8$) mice, and the concentrations of cytokines (G-CSF, IL-6) and chemokines (KC/CXCL-1, MCP-1) were measured by ELISA. **d** Footpads from WT ($n = 8$), *Ptpn6*^{spin} ($n = 8$) and *Ptpn6*^{spin}*Ets2*$^{fl/fl}$*LysM*$^{Cre+}$ ($n = 8$) mice were homogenized, and the concentrations of cytokines (G-CSF, IL-6) and chemokines (KC/CXCL-1, MCP-1) were measured by ELISA in the quantified lysates. Each point represents an individual mouse, and the lines represent the mean ± SD. The unpaired *t* test was used to determine the significance between the two groups analyzed. ns not significant; *$P < 0.05$; **$P < 0.01$; ***$P < 0.001$; ****$P < 0.0001$

radioimmunoprecipitation assay (RIPA) lysis buffer was used to collect cell lysates.

Histopathology

Mouse feet were preserved in formalin and then processed and paraffin-embedded following standard procedures. Paraffin blocks were then sectioned (5 µm width) and stained with hematoxylin and eosin (H&E). To stain for neutrophils specifically in the footpads, the paraffin blocks were sectioned (4 µm width), and slides were stained with anti-neutrophil antibody [7/4] (Novus Biologicals; NBP2-13077). Images were acquired by light microscopy with a Nikon Eclipse Ni Widefield Microscope.

Immunoblot analysis

To obtain protein lysates, footpad tissue was disrupted with a tissue homogenizer in RIPA lysis buffer supplemented with complete protease inhibitor cocktail (Roche) and PhosSTOP (Roche). Protein was quantified using the Pierce™ BCA Protein Assay Kit (Thermo Fisher Scientific) following the manufacturer's instructions. Sodium dodecyl sulfate polyacrylamide gel electrophoresis was used to resolve 40 µg of protein, which was then transferred to a polyvinylidene difluoride membrane. Next, the membrane was blocked in 5% nonfat milk and subjected to overnight incubation at 4 °C with primary antibody. After removal of the primary antibody, the membrane was incubated with horseradish peroxidase (HRP)-tagged secondary antibody for 1 h at room temperature. Finally, the Luminata™ Western HRP chemiluminescence substrate was added for visualization of stained proteins. Antibodies from Cell Signaling Technology (CST) were used to detect the following proteins: phospho-Erk1/2 (CST 9101), Erk1/2 (CST #9102), phospho-p38 (CST 9211), p38 (CST #9212), phospho-IκBα (CST #2859) and IκBα (CST #9242); the antibody to actin was from Proteintech (#66009-1-IG).

Microabrasion injury model

The microabrasion wound model has been described previously.[13] Briefly, 4–8-week-old, wild-type and disease-free *Ptpn6*^{spin} mice were anaesthetized. To irritate the hind paws and cause microabrasion (physical trauma and microinjuries), the plantar surfaces were gently rubbed with sterile sandpaper ten times. Then, the levels of proinflammatory molecules were measured in the footpads 6 h after wound induction.

In vivo cytokine levels

ELISA was used to measure cytokines in footpad protein lysates that were processed as described above or in serum.

ELISA

Cytokine ELISAs were performed per the manufacturer's instructions using the MCYTOMAG-70K kit (Millipore).

Quantitative PCR analysis

Total RNA was extracted using TRIzol (15596026, Thermo Fisher Scientific) and converted into cDNA by using the High-Capacity cDNA Reverse Transcription Kit (4368814, Applied Biosystems). Real-time quantitative PCR was performed on an ABI 7500 real-time PCR instrument with 2× SYBR Green PCR mix (4368706, Applied Biosystems). To determine the relative induction of cytokine mRNA in response to various stimuli, the mRNA expression level of each gene was normalized to the expression level of *Gapdh* mRNA. The following primer pairs were used for quantitative PCR analysis: Mm*Il1a* forward, 5′-AAAATCTCAGATTCA CAACTGTTCGT-3′, and reverse, 5′-TGGCAACTCCTTCAGCAACAC-3′; Mm*Mmp9* forward, 5′-GTCTTCCTGGGCAAGCAGTA-3′, and reverse, 5′-CTGGACAGAAACCCCACTTC-3′; Mm*Ccl3* forward, 5′-ACCATGACA CTCTGCAACCA-3′, and reverse, 5′-AGTCAGGAAAATGACACCTGG-3′; Mm*Ccl4* forward, 5′-TTCCTGCTGTTTCTCTTACACCT-3′, and reverse, 5′-CTGTCTGCCTCTTTTGGTCAG-3′; Mm*Il6* forward, 5′-GACAAAGCCA GAGTCCTTCAGAGAG-3′, and reverse, 5′-CTAGGTTTGCCGAGTAG ATCTC-3′; Mm*Tnf* forward, 5′-CATCTTCTCAAAATTCGAGTGACAA-3′, and reverse, 5′-TGGGAGTAGACAAGGTACAACCC-3′; Mm*Ifnb* forward, 5′-GCCTTTGCCATCCAAGAGATGC-3′, and reverse, 5′- ACACTG TCTGCTGGTGGAGTTC-3′; Mm*Syk* forward, 5′-CTACTACAAGGCCCA GACCC-3′, and reverse, 5′-TGATGCATTCGGGGGCGTAC-3′; Mm*Ets2* forward, 5′-GTGGCTTCCAAAAGGAGCAACG-3′, and reverse, 5′-TTCA CCAGGCTGAACTCGTTGG-3′; and Mm*Gapdh* forward, 5′-CGTCCCGT AGACAAAATGGT-3′, and reverse, 5′-TTGATGGCAACAATCTCCAC-3′. Error bars indicate the mean ± standard deviation (SD). The results are representative of at least two independent experiments.

Flow cytometry

Antibodies against Gr-1 (RB6-8C5) and CD11b (M1/70) were purchased from BioLegend and Invitrogen, respectively. Single-cell suspensions were prepared from the spleen and pLN by passing the suspensions through a cell strainer to remove cell debris. To deplete the red blood cells, an equal volume of ACK red blood cell lysis buffer was added to the cells and incubated at room temperature for 5 min. For staining, cells were washed in ice-cold flow cytometry buffer (0.5% (vol/vol) FCS and 2 mM EDTA in PBS, pH 7.5), incubated with each antibody for 30 min, washed twice and resuspended in the appropriate volume of flow cytometry buffer. Flow cytometry data were acquired on the LSR Fortessa or LSR II (BD Biosciences) and analyzed using FlowJo software (Tree Star).

Statistical analysis

All results are presented as the mean ± SD. Analysis of disease progress curves incorporated the log-rank (Mantel–Cox) test, and significant differences between two groups were determined by performing the Mann–Whitney test. Statistical analysis comparing multiple samples was performed with two-way ANOVA or unpaired *t* test. qPCR data were analyzed by the unpaired *t* test with Welch's correction. All analyses were performed using GraphPad Prism software (version 7.0). Differences were considered statistically significant when $P < 0.05$. ns, not significant; $^{*}P < 0.05$; $^{**}P < 0.01$; $^{***}P < 0.001$; $^{****}P < 0.0001$.

ACKNOWLEDGEMENTS

We would like to thank Dr. Yury Miller for the *Syk*$^{fl/fl}$ mice and Dr. Bruce Beutler for the *Ptpn6* mutant mice. We would like to thank the members of the Kanneganti lab for their comments and suggestions and Rebecca Tweedell, PhD, for scientific editing. This work was supported by the K22 NIAID Career Transition Award AI127836 to P.G., the National Institutes of Health grants CA163507, AR056296, AI124346 and AI101935 and by the American Lebanese Syrian Associated Charities to T.-D.K.

AUTHOR CONTRIBUTIONS

S.T. and T.-D.K. conceptualized the study; S.T. designed the experiments; S.T., P.G., R.K. and A.B. performed the experiments; P.H. provided *Ets2*$^{fl/fl}$ mice; and S.T. analyzed the data and wrote the paper. All authors critically evaluated and edited the paper and approved the final version. T.-D.K. oversaw the project.

ADDITIONAL INFORMATION

The online version of this article (https://doi.org/10.1038/s41423-020-0398-7) contains supplementary material.

Competing interests: The authors declare no competing interests.

REFERENCES

1. Cohen, P. R. Neutrophilic dermatoses: a review of current treatment options. *Am. J. Clin. Dermatol.* **10**, 301–312 (2009).
2. Callen, J. P. Neutrophilic dermatoses. *Dermatol. Clin.* **20**, 409–419 (2002).

3. Nesterovitch, A. B. et al. Alteration in the gene encoding protein tyrosine phosphatase nonreceptor type 6 (PTPN6/SHP1) may contribute to neutrophilic dermatoses. *Am. J. Pathol.* **178**, 1434–1441 (2011).
4. Eriksen, K. W. et al. Deficient SOCS3 and SHP-1 expression in psoriatic T cells. *J. Invest. Dermatol.* **130**, 1590–1597 (2010).
5. Christophi, G. P. et al. Macrophages of multiple sclerosis patients display deficient SHP-1 expression and enhanced inflammatory phenotype. *Lab. Invest.* **89**, 742–759 (2009).
6. Zhu, Z. et al. Tyrosine phosphatase SHP-1 in allergic and anaphylactic inflammation. *Immunol. Res.* **47**, 3–13 (2010).
7. Green, M. C. & Shultz, L. D. Motheaten, an immunodeficient mutant of the mouse. I. Genetics and pathology. *J. Hered.* **66**, 250–258 (1975).
8. Tsui, H. W., Siminovitch, K. A., de Souza, L. & Tsui, F. W. Motheaten and viable motheaten mice have mutations in the haematopoietic cell phosphatase gene. *Nat. Genet.* **4**, 124–129 (1993).
9. Nesterovitch, A. B. et al. Spontaneous insertion of a b2 element in the ptpn6 gene drives a systemic autoinflammatory disease in mice resembling neutrophilic dermatosis in humans. *Am. J. Pathol.* **178**, 1701–1714 (2011).
10. Croker, B. A. et al. Inflammation and autoimmunity caused by a SHP1 mutation depend on IL-1, MyD88, and a microbial trigger. *Proc. Natl Acad. Sci. USA* **105**, 15028–15033 (2008).
11. Pao, L. I., Badour, K., Siminovitch, K. A. & Neel, B. G. Nonreceptor protein-tyrosine phosphatases in immune cell signaling. *Annu Rev. Immunol.* **25**, 473–523 (2007).
12. Gurung, P. et al. Tyrosine kinase SYK licenses MyD88 adaptor protein to instigate IL-1alpha-mediated inflammatory disease. *Immunity* **46**, 635–648 (2017).
13. Lukens, J. R. et al. RIP1-driven autoinflammation targets IL-1alpha independently of inflammasomes and RIP3. *Nature* **498**, 224–227 (2013).
14. Tartey, S., Gurung, P., Dasari, T. K., Burton, A. & Kanneganti, T. D. ASK1/2 signaling promotes inflammation in a mouse model of neutrophilic dermatosis. *J. Clin. Invest.* **128**, 2042–2047 (2018).
15. Tartey, S., Gurung, P., Samir, P., Burton, A. & Kanneganti, T. D. Cutting Edge: dysregulated CARD9 signaling in neutrophils drives inflammation in a mouse model of neutrophilic dermatoses. *J. Immunol.* **201**, 1639–1644 (2018).
16. Abram, C. L., Roberge, G. L., Pao, L. I., Neel, B. G. & Lowell, C. A. Distinct roles for neutrophils and dendritic cells in inflammation and autoimmunity in motheaten mice. *Immunity* **38**, 489–501 (2013).
17. Mocsai, A., Ruland, J. & Tybulewicz, V. L. The SYK tyrosine kinase: a crucial player in diverse biological functions. *Nat. Rev. Immunol.* **10**, 387–402 (2010).
18. Mocsai, A., Zhou, M., Meng, F., Tybulewicz, V. L. & Lowell, C. A. Syk is required for integrin signaling in neutrophils. *Immunity* **16**, 547–558 (2002).
19. Mocsai, A. et al. G-protein-coupled receptor signaling in Syk-deficient neutrophils and mast cells. *Blood* **101**, 4155–4163 (2003).
20. Zhong, X., Chen, B., Yang, L. & Yang, Z. Molecular and physiological roles of the adaptor protein CARD9 in immunity. *Cell Death Dis.* **9**, 52 (2018).
21. Roth, S. & Ruland, J. Caspase recruitment domain-containing protein 9 signaling in innate immunity and inflammation. *Trends Immunol.* **34**, 243–250 (2013).
22. Ghosh, D., Tsokos, G. C. & Kyttaris, V. C. c-Jun and Ets2 proteins regulate expression of spleen tyrosine kinase in T cells. *J. Biol. Chem.* **287**, 11833–11841 (2012).
23. Krishnan, S. et al. Differential expression and molecular associations of Syk in systemic lupus erythematosus T cells. *J. Immunol.* **181**, 8145–8152 (2008).
24. Wei, G. et al. Activated Ets2 is required for persistent inflammatory responses in the motheaten viable model. *J. Immunol.* **173**, 1374–1379 (2004).
25. Tecchio, C., Micheletti, A. & Cassatella, M. A. Neutrophil-derived cytokines: facts beyond expression. *Front. Immunol.* **5**, 508 (2014).
26. Di Paolo, N. C. & Shayakhmetov, D. M. Interleukin 1alpha and the inflammatory process. *Nat. Immunol.* **17**, 906–913 (2016).
27. Rider, P. et al. IL-1alpha and IL-1beta recruit different myeloid cells and promote different stages of sterile inflammation. *J. Immunol.* **187**, 4835–4843 (2011).
28. Quinn, S. R. et al. The role of Ets2 transcription factor in the induction of microRNA-155 (miR-155) by lipopolysaccharide and its targeting by interleukin-10. *J. Biol. Chem.* **289**, 4316–4325 (2014).
29. Tonks, N. K. Protein tyrosine phosphatases: from genes, to function, to disease. *Nat. Rev. Mol. Cell Biol.* **7**, 833–846 (2006).
30. Cao, H. & Hegele, R. A. Identification of polymorphisms in the human SHP1 gene. *J. Hum. Genet.* **47**, 445–447 (2002).
31. Christophi, G. P. et al. SHP-1 deficiency and increased inflammatory gene expression in PBMCs of multiple sclerosis patients. *Lab. Invest.* **88**, 243–255 (2008).
32. Dubois, M. J. et al. The SHP-1 protein tyrosine phosphatase negatively modulates glucose homeostasis. *Nat. Med.* **12**, 549–556 (2006).
33. Geraldes, P. et al. Activation of PKC-delta and SHP-1 by hyperglycemia causes vascular cell apoptosis and diabetic retinopathy. *Nat. Med.* **15**, 1298–1306 (2009).
34. Robinson, M. J. et al. Dectin-2 is a Syk-coupled pattern recognition receptor crucial for Th17 responses to fungal infection. *J. Exp. Med.* **206**, 2037–2051 (2009).
35. Gringhuis, S. I. et al. Dectin-1 directs T helper cell differentiation by controlling noncanonical NF-kappaB activation through Raf-1 and Syk. *Nat. Immunol.* **10**, 203–213 (2009).
36. Yamada, T. et al. IL-1 induced chemokine production through the association of Syk with TNF receptor-associated factor-6 in nasal fibroblast lines. *J. Immunol.* **167**, 283–288 (2001).
37. Baran, C. P. et al. Transcription factor ets-2 plays an important role in the pathogenesis of pulmonary fibrosis. *Am. J. Respir. Cell Mol. Biol.* **45**, 999–1006 (2011).
38. Trojanowska, M. Ets factors and regulation of the extracellular matrix. *Oncogene* **19**, 6464–6471 (2000).
39. Yang, H. et al. ETS family transcriptional regulators drive chromatin dynamics and malignancy in squamous cell carcinomas. *Elife* **4**, e10870 (2015).
40. Sementchenko, V. I. & Watson, D. K. Ets target genes: past, present and future. *Oncogene* **19**, 6533–6548 (2000).
41. Yamamoto, H. et al. Defective trophoblast function in mice with a targeted mutation of Ets2. *Genes Dev.* **12**, 1315–1326 (1998).
42. Saijo, K. et al. Essential role of Src-family protein tyrosine kinases in NF-kappaB activation during B cell development. *Nat. Immunol.* **4**, 274–279 (2003).
43. Pao, L. I. et al. B cell-specific deletion of protein-tyrosine phosphatase Shp1 promotes B-1a cell development and causes systemic autoimmunity. *Immunity* **27**, 35–48 (2007).
44. Clausen, B. E., Burkhardt, C., Reith, W., Renkawitz, R. & Forster, I. Conditional gene targeting in macrophages and granulocytes using LysMcre mice. *Transgenic Res.* **8**, 265–277 (1999).
45. Passegue, E., Wagner, E. F. & Weissman, I. L. JunB deficiency leads to a myeloproliferative disorder arising from hematopoietic stem cells. *Cell* **119**, 431–443 (2004).